

Influence of substrate temperature on the properties of electron beam evaporated ZnSe films

M. G. Syed Basheer Ahamed¹, V. S. Nagarethinam², A. R. Balu², A. Thayumanavan², K. R. Murali³, C. Sanjeeviraja⁴, and M. Jayachandran^{*3}

¹ MIET Arts and Science College, Trichy – 620 007, India

² Department of Physics, A.V.V.M Sri Pushpam College, Poondi, India

³ Electrochemical Materials Science Division, Central Electrochemical Research Institute, Karaikudi – 630 006, (Council of Scientific and Industrial Research, New Delhi), India

⁴ Department of Physics, Alagappa University, Karaikudi-630 003, India

Received 16 October 2009, revised 11 January 2010, accepted 14 January 2010

Published online 29 January 2010

Key words ZnSe, II-VI, thin films, semiconductor.

ZnSe films were deposited on glass substrates keeping the substrate temperatures, at room temperature (RT), 75, 150 and 250 °C. The films have exhibited cubic structure oriented along the (111) direction. Both the crystallinity and the grain size increased with increasing deposition temperature. A very high value of absorption co-efficient (10^4 cm^{-1}) is observed. The band gap values decrease from a value of 2.94 eV to 2.69 eV with increasing substrate temperature. The average refractive index value is in the range of 2.39 – 2.41 for the films deposited at different substrate temperatures. The conductivity values increases continuously with temperature. Laser Raman spectra showed peaks at 140.8 cm^{-1} , 246.7 cm^{-1} and 204.5 cm^{-1} which are attributable to 2TA LO phonon and TO phonon respectively.

© 2010 WILEY-VCH Verlag GmbH & Co. KGaA, Weinheim

1 Introduction

Polycrystalline zinc selenide (ZnSe) thin film is an important promising material for optoelectronic devices such as light emitting diodes, ultrasonic transducers, photodetectors [1]. Due to larger direct band gap around 2.7 eV at room temperature, ZnSe thin film have also attracted considerable interest in their applications in photovoltaic devices, for instance, ZnSe has been used to increase the open circuit voltage of solar cells [2]. Recently, ZnSe becomes an attractive material as the window layer of CuInSe₂ based solar cells [3].

ZnSe film has been prepared by various growth techniques, such as molecular beam epitaxy (MBE) [4], metalorganic chemical vapour deposition (MOCVD) [5], atomic layer epitaxy (ALE) [6], electro-deposition [7], chemical bath deposition [8], photochemical [9], spray pyrolysis [10], and thermal evaporation [11]. In addition, advances in low temperature epitaxial growth techniques such as MBE and MOCVD had been demonstrated to achieve high quality II–VI compound semiconductor films. The substrate temperature of ZnSe film grown by MBE was reported in the range from 250 °C to 450 °C [12].

In order to lower the production cost and to realize large-scale production, ZnSe films have been deposited on various substrates, such as ITO glass [13], glass [14], silicon [15] and silica substrates [16]. Currently, ZnSe film deposited on glass substrate becomes a very promising issue for optoelectronic application. The device performance has been demonstrated to be influenced by the structural properties of the deposited film [17]. The structural parameters such as the crystallinity, lattice constant, grain size, strain, dislocation density and crystal orientation depend strongly on the growth conditions such as growth temperature and Se/Zn ratio [18]. Recently, the influence of substrate temperature on compositional, structural, optical and electrical properties of polycrystalline ZnSe films has been reported [11], and the influence of Se/Zn ratio on the grain size and photo-conducting properties has also been investigated [19]. In this paper, ZnSe film has been deposited on glass substrates by the Electron beam evaporation (EBE) technique. The growth of ZnSe films is carried out as

* Corresponding author: e-mail: mjayam54@yahoo.com

a function of substrate temperature and the films were characterized for their structural, optical, electrical and surface morphological properties.

2 Experimental

ZnSe films were deposited on glass substrates maintaining the temperatures at RT, 75, 150 and 250 °C. Substrate temperature was selected from the analysis of the TGA result of the ZnSe powder. The vacuum was 10^{-6} Torr during deposition of the films. Film thickness was measured by the stylus Profilometer (Mitutoyo). Crystallinity and orientation of the films were studied by X-ray diffraction (XRD) analysis using $\text{CuK}\alpha$ radiation from an Xpert pro PANalytical XRD unit. Optical transmission spectra were recorded at room temperature using a UV-Vis-NIR spectrophotometer. Surface morphological studies were conducted by using a Molecular Imaging system atomic force microscope. Laser Raman spectra were recorded using Renishaw InVia Laser Raman microscope using a 18 mW 633 nm He – Ne laser. Electrical resistivity measurements were performed by making aluminium (Al) contacts.

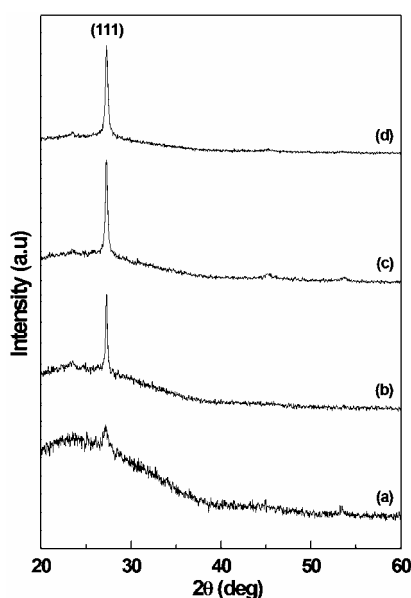


Fig. 1 XRD patterns for the ZnSe films deposited at different substrate temperatures (a) RT (b) 75 °C (c) 150 °C (d) 250 °C.

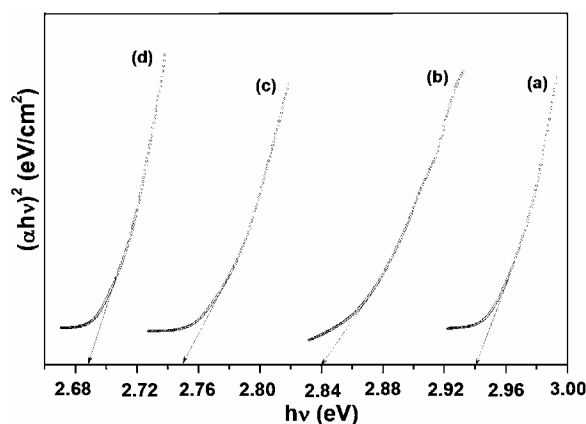


Fig. 2 $(\alpha hv)^2$ vs $h\nu$ plot for the ZnSe films deposited at different substrate temperatures (a) RT (b) 75 °C (c) 150 °C (d) 250 °C.

Table 1 Lattice parameter, Grain size, strain, stress and dislocation density of ZnSe films deposited at different substrate temperatures.

Substrate Temp (°C)	Thickness (nm)	Lattice parameter a (Å)	Grain size (nm)	stress dyne cm^{-2} ($\times 10^{10}$)	strain ($\times 10^{-4}$)	dislocation density ($\times 10^{16} \text{cm}^{-3}$)
R.T	220	5.576	12.2	0.061	2.82	61.12
75	235	5.561	17.1	0.134	2.01	32.01
150	224	5.642	21.6	-0.074	1.61	21.00
250	240	5.647	32.8	-0.072	1.10	9.36

3 Results and discussion

X-ray diffraction studies indicated that the films are polycrystalline having the fcc zinc blende structure irrespective of the substrate temperature. Figure 1 shows the XRD pattern of the films deposited at different substrate temperatures. It is observed that the films exhibit highly preferred orientation along the (111) direction. No other peaks are observed which confirms the formation of single phase ZnSe. The associated

micro structural parameters for the ZnSe films deposited at different temperature are presented in table 1. The deviation in the lattice parameter values from the bulk value observed in the present case clearly suggests that the grains in the films are under stress. Such behaviour can be attributed to the change of nature, deposition conditions and the concentration of the native imperfections developed in thin films. This results in either elongation or compression of the lattice and the structural parameters. The density of the film is therefore found to change considerably in accordance with the variations observed with the lattice constant values [20,21]. The increase of lattice parameter with increase of substrate temperature suggests that the grains were strained in the as-deposited film possibly due to the appreciable concentration of the native imperfections.

The grain size is observed to increase from about 12 to 32 nm with substrate temperature. The stress developed at higher substrate temperatures is likely to be due to the formation of native defects developed from the lattice misfit or dislocations. The defects have a probability to migrate parallel to the substrate surface with the surface mobility greatly influenced by the substrate temperature so that the films will have a tendency to expand and develop an internal tensile stress. This type of change in internal stress is always predominant by the observed recrystallization process in polycrystalline films. The stress relaxation is mainly considered as due to dislocation glides formed in the evaporated films. The decrease of internal stress beyond 75 °C may be attributed to a decrease in dislocation density. It is observed that the microstrain variation exhibits a slow decreasing trend up to 75 °C and decreases afterwards with further increase of substrate temperature. The reduction in the strain and dislocation density with substrate temperature may be due to the movement of interstitial Zn atoms from the bulk of the grain to its boundary region which dissipate to larger area leading to reduction in concentration of lattice imperfections. Similar trend has been observed earlier [11,18].

The degree of preferred orientation in cubic ZnSe thin films can be assessed by calculating ratio of the peak intensity of (111) plane to the intensity of (220) plane. The degree of preferred orientation of the films is found to decrease when the internal stress and microstrain are stronger. Similar behaviour is observed with increasing dislocation density. Such behaviour shows the degree of preferred orientation is the measuring index given the essential characteristics of the inherent defect states. An increase in the height of the XRD peak indicates preferred orientation which in turn is expected to enhance considerably the reduction process of the imperfections originating from lattice misfit in the EB evaporated ZnSe films. Venkatasubbaiah et al. [22] have observed the same defect characteristics for the ZnSe films prepared by the close space evaporation technique. A close analysis of the dependence of the above microstructural parameters on the substrate temperature indicates that the degree of preferred orientation along with the other microstructural features are more prominent than the crystallite size for films with low thickness. This type of correlation is observed and reported by earlier workers [18,23] for other II-VI thin films like CdSe as well.

The optical properties were studied by recording the transmittance and absorption spectra of these ZnSe films in the wavelength range 400 – 2000 nm. The sharp rise in the absorption curve below 500nm confirms the highly crystalline and monophase nature of the deposited films. The absorption co-efficient (α) values calculated from the transmittance data are about 10^4 cm^{-1} near the absorption edge as well as in the visible region. A plot of $(\alpha h\nu)^2$ vs $h\nu$ (Fig. 2) is linear the absorption edge confirming the direct band gap transition in ZnSe films. Extrapolating the straight line portion of these plots to the $h\nu$ axis and from the point of intersection on the $h\nu$ axis, band gap values in the range 2.94 – 2.69 eV are observed for the films deposited at different substrate temperatures. The band gap values are blue shifted from the standard value of E_g (bulk) (2.60 – 2.70 eV). This may be attributed to the increase of crystallinity and highly oriented nature as well as to the reduced crystallite size of the deposited films. As the substrate temperature increased the crystallite size also increases as revealed from XRD studies. The red shift in the absorption edge with increase in grain size can be assigned to the quantum size effect. Such a red shift has been reported for chemically deposited ZnSe [24]. The red shift in the bandgap with increase of particle size can be predicted by the three dimensional confinement model based on effective mass approximation [25] $\Delta E_g = E_g^{\text{eff}} - h^2\pi^2/2\mu R^2$, where, $1/\mu = (1/m_e^* + 1/m_h^*)$, where E_g^{eff} is the effective band gap energy, E_g is the bulk band gap energy, R is the particle radius, h is the Planck constant, μ is the reduced effective mass and m_e^* and m_h^* are the electron and hole effective masses respectively.

The optical transmittance variation (Fig. 3) was studied in the wavelength range of 400 – 2000 nm for the films deposited at different substrate temperature. The transmittance spectra exhibit interference fringes. The refractive index was calculated from the transmission spectra by the envelope method [26] using the following equations:

$$n = [N + (N^2 - n_s^2)]^2 \quad (1)$$

$$N = (n_s^2 + 1)/2 + 2n_s(T_{\max} - T_{\min})/T_{\max} T_{\min} \quad (2)$$

where n_s is the refractive index of the substrate, T_{\max} and T_{\min} are the maximum and minimum transmittances at the same wavelength in the fitted envelope curve on a transmittance spectrum. Figure 4 shows the variation of the refractive index for the films deposited at different substrate temperatures. The refractive index is nearly constant about 2.39 – 2.41 in the visible region. Beyond the absorption edge region, there is a sharp rise in the refractive index value. However, a small increase is observed in the average refractive index values for the films deposited at higher temperatures. This can be attributed to the improved crystallinity of the ZnSe films at higher temperatures. The value of the refractive index is comparable with the value of 2.457 reported for vacuum evaporated films [17].

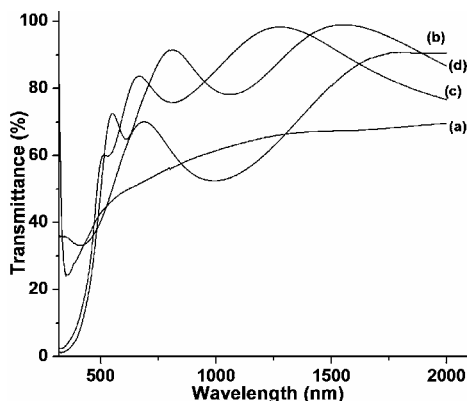


Fig. 3 Optical transmittance behaviour of ZnSe films deposited at different substrate temperatures (a) RT (b) 75 °C (c) 150 °C (d) 250 °C.

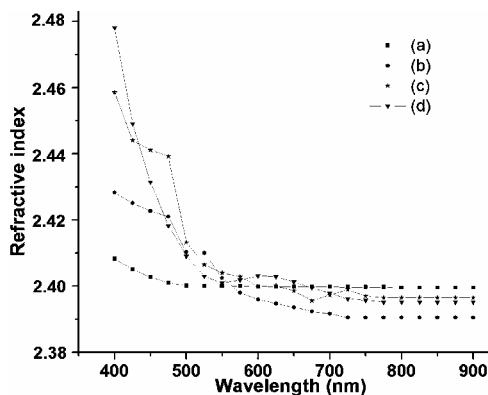


Fig. 4 Refractive index graph for the ZnSe films deposited at different substrate temperatures a) RT b) 75 °C c) 150 °C and d) 250 °C.

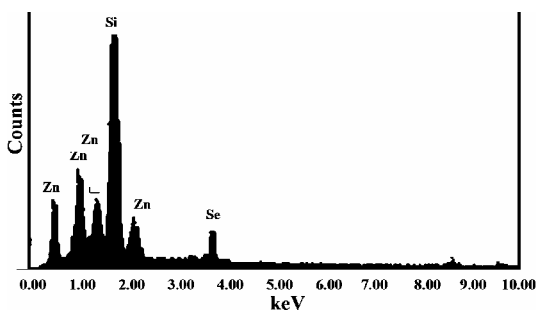


Fig. 5 EDAX spectrum for the ZnSe films deposited at a substrate temperature of 250 °C.

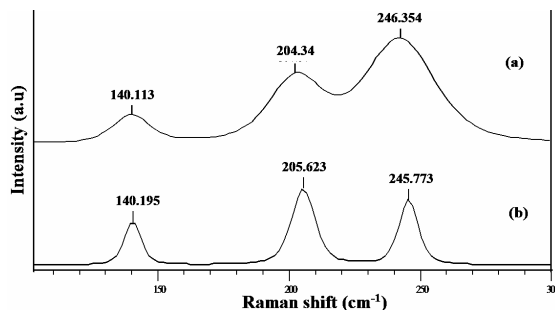


Fig. 7 Raman spectra for the ZnSe films deposited at different substrate temperatures (a) RT and (b) 250 °C.

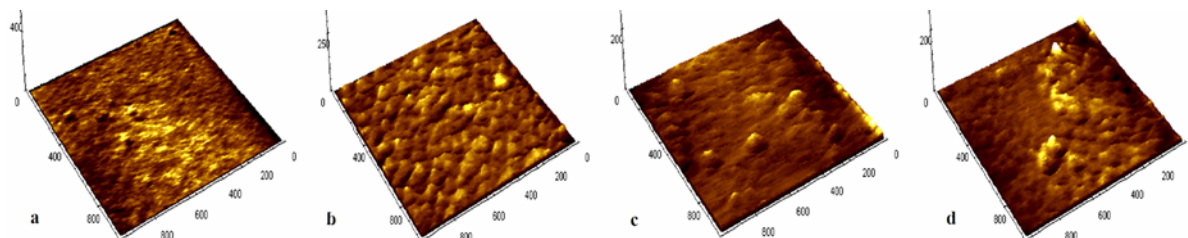


Fig. 6 Three dimensional (3D) topographic AFM images of ZnSe films deposited at different substrate temperatures (a) RT (b) 75 °C (c) 150 °C (d) 250 °C. (Online color at www.crt-journal.org)

Compositional analysis was done for the films deposited at different substrate temperatures. Figure 5 shows the EDAX spectrum of the films deposited at 250 °C. The films deposited at room temperature (RT) had a selenium rich composition (Zn: 45.1% and Se : 54.9 %), as the substrate temperature increased the composition changed to zinc side. For the films deposited at 250 °C, the composition was Zn: 51.0%, Se: 49.0 %. The

silicon peak is due to the silica glass substrate. This value is in agreement with the data on chemically deposited ZnSe films [24].

When a temperature gradient is maintained at the opposite ends of a semiconductor film, thermo power is generated, due to which a thermo emf (electromotive force) is developed. The temperature difference maintained at the two ends of the film tends to drive the majority carriers from the hot end to the cold end. This is the cause of the thermo emf. The semiconductor is placed on a metal plate (also films deposited on either conducting substrates or non-conducting substrates) and a heated metal is connected to the metal base through a multimeter. One end of the metal base, which is connected to the multimeter, is called the cold junction and the hot tip is the hot junction. When the semiconductor is momentarily touched with the hot probe, the current flows from the cold junction to the hot junction for n-type semiconductor and for the p-type, current flows from the hot to the cold junction. The results of this study indicates that the ZnSe films deposited by the EB evaporation technique exhibit p-type behaviour.

Figure 6 shows the atomic force microscopic images of the EB evaporated films deposited at different substrate temperatures. The films exhibit a uniform surface with fine grains. The average value of surface roughness is about 0.12 nm. As the substrate temperature increased the grain size also increased with a coarse morphology. The grain size is observed to increase from about 25 nm to 65 nm as the substrate temperature increased from 30 °C to 250 °C. The surface roughness also increased to 0.67 nm for the films deposited at higher substrate temperatures. The grain size obtained by the EB evaporation technique is lower than those obtained by thermal vacuum evaporation [27].

The values of resistivity of the films are in the range of $10^6 \Omega\text{cm}$. This high resistivity is due to the excess selenium present in the films. The value reduces to $3.05 \times 10^5 \Omega\text{cm}$ as the substrate temperature increased to 250 °C. This is due to decrease in selenium content in the ZnSe films deposited at higher temperatures as evident from EDAX studies. The value of resistivity is lower than the resistivity values obtained with thermally evaporated and chemically deposited ZnSe films [27,28].

The Raman spectra of the films exhibit LO and TO phonons at 246.7 cm^{-1} and 204.5 cm^{-1} . The intensity of the peaks increased with substrate temperature. Figure 7 shows the Raman spectrum of the films deposited at RT and 250 °C. A peak corresponding to 2TA is also observed at 140.8 cm^{-1} . Similar observations were reported earlier by Lu et al [26]. From previous reports, the LO phonon frequency of crystalline ZnSe films was 254 cm^{-1} and that of single crystal ZnSe was 255 cm^{-1} at room temperature and for ZnSe polycrystalline nanoparticles, the TO and LO phonon frequencies were observed at 210 and 255 cm^{-1} respectively, and exhibit a broad Raman peak due to the high surface to volume ratio of small particles [30]. In this work, the LO and TO phonon peaks of the ZnSe films are shifted towards the lower frequency, which may be due to the effect of small size.

4 Conclusions

The results of this study indicate that uniform and device quality ZnSe films with cubic structure can easily be deposited by the EB evaporation technique. Films with direct band gap in the range of 2.69 – 2.94 eV can be deposited. Films with grain size in the range 25 – 65 nm can be obtained. Thus the EB evaporation technique possesses the advantage of growing ZnSe films with nanocrystalline grains and low resistivity compared to the thermal vacuum evaporation technique.

References

- [1] T. Shirakawa, Mater. Sci. Eng. B **91- 92**, 470 (2002).
- [2] T. L. Chu and S. S. Chu, Prog. Photovolt. Res. Appl. **1**, 31 (1993).
- [3] A. Nouhi and R. J. Stirn, Solar Cells **21**, 225 (1987).
- [4] J. S. Song, J. H. Chang, D. C. Oh, J. J. Kim, M. W. Cho, and H. Makino, J Cryst. Growth **249**, 128 (2003).
- [5] K. Morimoto, J. Appl. Phys. **66**, 4206 (1989).
- [6] C. D. Lee, S. L. Min, and S. K. Chang, J. Cryst. Growth **159**, 108 (1996).
- [7] G. Riveros, H. Gomez, R. Henriquez, R. Schrebler, R. E. Marotti, and E. A. Dalchiele, Sol. Energy Mater. Sol. Cells **70**, 255 (2001).
- [8] A. M. Chaparro, M. A. Martinez, C. Guillen, R. Bayon, M. T. Gutierrez, and J. Herrero, Thin Solid Films **361 - 362**, 177 (2000).

- [9] R. Kumaresan, M. Ichimura, and E. Arai, *Thin Solid Films* **414**, 25 (2002).
- [10] M. Bedir, M. Oztas, O. F. Bakkaloglu, and R. Ormanci, *J. Eur. Phys. B* **45**, 465 (2005).
- [11] S. Venkatachalam, D. Mangalaraj, Sa. K. Narayandass, K. Kim, and J. Yi, *Physica B* **358**, 27 (2005).
- [12] J. M. DePuydt, H. Cheng, J. E. Potts, T. L. Smith, and S. K. Mohapatra, *J Appl. Phys.* **62**, 4756 (1987).
- [13] C. T. Hsu, Y. K. Su, T. S. Wu, and M. Yokoyama, *Jpn. J. Appl. Phys.* **33**, 161 (1994).
- [14] M. Singh and Y. K. Vijay, *Appl. Surf. Sci.* **239**, 79 (2004).
- [15] M. Yokoyama, N. T. Chen, and H. Y. Ueng, *J. Cryst. Growth* **212**, 97 (2000).
- [16] E. E. Khawaja, S. M. A. Durrani, A. B. Hallak, M. A. Salim, and M. S. Hussain, *J. Phys. D* **27**, 1008 (1994).
- [17] S. Venkatachalam, D. Mangalaraj, Sa. Ka. Narayandass, K. Kim, and J. Yi, *Vacuum* **81**, 928 (2007).
- [18] P. K. Kalita, B. K. Sarma, and H. L. Das, *Bull. Mater. Sci.* **23**, 313 (2000).
- [19] M. Oztas, M. Bedir, O. F. Bakkaloglu, and R. Ormanci, *Acta Phys. Pol. A* **107**, 525 (2005).
- [20] M. El. Sherrif, F. S. Terra, and S. A. Khodier, *J. Mater. Sci. Mater. Electron.* **7**, 391 (1996).
- [21] K. Reichelt and X. Jiang, *Thin Solid Films* **191**, 150 (1995).
- [22] Y. P. Venakatasubbaiah, P. Pratap, M. Devika, and K. T. Ramakrishna Reddy, *Physica B* **165**, 240 (2005).
- [23] A. Ashor, N. El-Kadry, M. R. Ebid, M. Farghal, and A. A. Ramadan, *Thin Solid Films* **279**, 242 (1996).
- [24] R. B. Kale and C. D. Lokhande, *Appl. Surf. Sci.* **252**, 929 (2005).
- [25] P. K. Kuirri, H. P. Lenka, J. Ghatak, G. Sahu, B. Joseph, and D. P. Mahapatra, *J. Appl. Phys.* **102**, 024315 (2007).
- [26] H. Y. Joo and H. J. Kim, *J. Vac. Sci. Technol. A* **17**, 862 (1999).
- [27] E. Bacaksiz, S. Aksub, I. Polat, S. Yilmaza, and M. Altunbas, *J. Alloys Comp.* **487**, 280 (2009).
- [28] C. Mehta, G. S. S. Saini, J. M. Abbas, and S. K. Tripathi, *Appl. Surf. Sci.* **256**, 608 (2009).
- [29] G. Lu, H. An, Y. Chen, J. Huang, H. Zhang, B. Ziang, Q. Zhao, D. Yu, and W. Du, *J. Cryst. Growth* **274**, 530 (2005).
- [30] D. Sarigiannis, J. D. Pack, G. Kioseoglou, A. Petrou, and T. J. Mountziaris, *Appl. Phys. Lett.* **80**, 4024 (2002).